

Enlarging minimal-Supergravity parameter space by decreasing pre-Nucleosynthesis Hubble rate in Scalar-Tensor Cosmologies

Riccardo Catena,^{1,*} Nicolao Fornengo,^{2,3,†} Antonio Masiero,^{4,5,‡} Massimo Pietroni,^{5,§} and Mia Schelke^{3,¶}

¹*Scuola Internazionale Superiore di Studi Avanzati
Via Beirut 2-4, I-34014 Trieste, Italy*

²*Dipartimento di Fisica Teorica, Università di Torino
via P. Giuria 1, I-10125 Torino, Italy*

³*Istituto Nazionale di Fisica Nucleare, Sezione di Torino
via P. Giuria 1, I-10125 Torino, Italy*

⁴*Dipartimento di Fisica, Università di Padova
via Marzolo 8, I-35131, Padova, Italy*

⁵*Istituto Nazionale di Fisica Nucleare, Sezione di Padova
via Marzolo 8, I-35131, Padova, Italy*

(Dated: February 2, 2008)

We determine under what conditions Scalar Tensor cosmologies predict an expansion rate which is reduced as compared to the standard General Relativity case. We show that ST theories with a single matter sector typically predict an enhanced Hubble rate in the past, as a consequence of the requirement of an attractive fixed point towards General Relativity at late times. Instead, when additional matter sectors with different conformal factors are added, the late time convergence to General Relativity is maintained and at the same time a reduced expansion rate in the past can be driven. For suitable choices of the parameters which govern the scalar field evolution, a sizeable reduction (up to about 2 orders of magnitude) of the Hubble rate prior to Big Bang Nucleosynthesis can be obtained. We then discuss the impact of these cosmological models on the relic abundance of dark matter in minimal Supergravity models: we show that the cosmologically allowed regions in parameter space are significantly enlarged, implying a change in the potential reach of LHC on the neutralino phenomenology.

PACS numbers: 95.35.+d, 95.36.+x, 98.80.-k, 04.50.+h, 98.80.Cq

I. CHANGING THE EXPANSION RATE IN THE PAST

In a standard flat FRW universe described by GR, the expansion rate of the universe, $H_{GR} \equiv \dot{a}/a$, is set by the total energy density, $\tilde{\rho}_{\text{tot}}$, according to the Friedmann law,

$$H_{GR}^2 = \frac{1}{3M_p^2} \tilde{\rho}_{\text{tot}}, \quad (1)$$

where M_p is the Planck mass, related to the Newton constant by $M_p = (8\pi G)^{-1/2}$. If the total energy density is dominated by relativistic degrees of freedom, the expansion rate is related to the temperature through the relation

$$H_{GR} \simeq 1.66 g_*^{1/2} \frac{T^2}{M_p}, \quad (2)$$

with g_* the effective number of relativistic degrees of freedom (see for instance [1]).

In order to modify the above $H-T$ relation, one can do one (or more) of the following:

- 1) change the number of relativistic d.o.f.'s, g_* ;
- 2) consider a $\tilde{\rho}_{\text{tot}}$ not dominated by relativistic d.o.f.'s;
- 3) consider a modification of GR in which an effective Planck mass, different from M_p appears in (2).

One example of a scenario of the first type is obtained by adding N extra light neutrino families to the standard model, which increases g_* by $7/4 N$.

The second situation is realized *e.g.* in the so called “kination” scenario [2], where the energy density at a certain epoch is dominated by the kinetic energy of a scalar field. Since the kinetic energy redshifts as $\rho_{\text{kin}} \sim a^{-6}$, it will eventually become subdominant with respect to radiation ($\rho_{\text{rad}} \sim a^{-4}$). As long as ρ_{kin} dominates, the expansion rate is bigger than in the “standard” scenario where there is no scalar field and the same amount of radiation.

In this paper we will consider scenarios of the third type, where the expansion rate is modified by changing the effective gravitational coupling. This can be realized in a fully covariant way in ST theories [3]. We will consider the class of ST theories which can be defined by the following action [4],

$$S = S_g + \sum_i S_i, \quad (3)$$

*Electronic address: catena@sissa.it

†Electronic address: fornengo@to.infn.it

‡Electronic address: masiero@pd.infn.it

§Electronic address: pietroni@pd.infn.it

¶Electronic address: schelke@to.infn.it

where S_g is the gravitational part, given by the sum of the Einstein-Hilbert and the scalar field actions,

$$S_g = \frac{M_*^2}{2} \int d^4x \sqrt{-g} \left[R + g^{\mu\nu} \partial_\mu \varphi \partial_\nu \varphi - \frac{2}{M_*^2} V(\varphi) \right], \quad (4)$$

where $V(\varphi)$ can be either a true potential or a (Einstein frame) cosmological constant, $V(\varphi) = V_0$. The S_i 's are the actions for separate “matter” sectors

$$S_i = S_i[\Psi_i, A_i^2(\varphi) g_{\mu\nu}], \quad (5)$$

with Ψ_i indicating a generic field of the i -th matter sector, coupled to the metric $A_i^2(\varphi) g_{\mu\nu}$. The actions S_i are constructed starting from the Minkowski actions of Quantum Field Theory, for instance the SM or the MSSM ones, by substituting the flat metric $\eta_{\mu\nu}$ everywhere with $A_i^2(\varphi) g_{\mu\nu}$.

The emergence of such a structure, with different conformal factors A_i^2 for the various sectors can be motivated in extra-dimensional models, assuming that the two sectors live in different portions of the extra-dimensional space. A similar structure, leading to more dark matter species, each with a different conformal factor, was considered in [5].

We consider a flat FRW space-time

$$ds^2 = dt^2 - a^2(t) dl^2,$$

where the matter energy-momentum tensors, $T_{\mu\nu}^i \equiv 2(-g)^{-1/2} \delta S_i / \delta g^{\mu\nu}$ admit the perfect-fluid representation

$$T_{\mu\nu}^i = (\rho_i + p_i) u_\mu u_\nu - p_i g_{\mu\nu}, \quad (6)$$

with $g_{\mu\nu} u^\mu u^\nu = 1$.

The cosmological equations then take the form

$$\frac{\ddot{a}}{a} = -\frac{1}{6M_*^2} \left[\sum_i (\rho_i + 3p_i) + 2M_*^2 \dot{\varphi}^2 - 2V \right], \quad (7)$$

$$\left(\frac{\dot{a}}{a} \right)^2 = \frac{1}{3M_*^2} \left[\sum_i \rho_i + \frac{M_*^2}{2} \dot{\varphi}^2 + V \right], \quad (8)$$

$$\ddot{\varphi} + 3\frac{\dot{a}}{a}\dot{\varphi} = -\frac{1}{M_*^2} \left[\sum_i \alpha_i (\rho_i - 3p_i) + \frac{\partial V}{\partial \varphi} \right], \quad (9)$$

where the coupling functions α_i are given by

$$\alpha_i \equiv \frac{d \log A_i}{d\varphi}. \quad (10)$$

The Bianchi identity holds for each matter sector separately, and reads,

$$d(\rho_i a^3) + p_i da^3 = (\rho_i - 3p_i) a^3 d \log A_i(\varphi), \quad (11)$$

implying that the energy densities scale as

$$\rho_i \sim A_i(\varphi)^{1-3w_i} a^{-3(1+w_i)}, \quad (12)$$

with $w_i \equiv p_i/\rho_i$ the equation of state associated to the i -th energy density (assuming w_i is constant).

A. GR as a fixed point

To start, consider the case of a single matter sector, S_M . In order to compare the ST case with the GR one of Eqs. (1, 2), it is convenient to Weyl-transform to the so-called Jordan Frame (JF), where the energy-momentum tensor is covariantly conserved. The transformation amounts to a rescaling of the metric according to

$$\tilde{g}_{\mu\nu} = A_M^2(\varphi) g_{\mu\nu}, \quad (13)$$

keeping the comoving spatial coordinates and the conformal time $dt = dt/a$ fixed [6]. The JF matter energy-momentum tensor, $\tilde{T}_{\mu\nu}^M \equiv 2(-\tilde{g})^{-1/2} \delta S_M / \delta \tilde{g}^{\mu\nu}$, is related to that in eq. (6) by $\tilde{T}_{\mu\nu}^M = A_M^{-2} T_{\mu\nu}^M$, so that energy density and pressure transform as

$$\tilde{\rho}_M = A_M^{-4} \rho_M, \quad \tilde{p}_M = A_M^{-4} p_M, \quad (14)$$

while the cosmic time transforms as $d\tilde{t} = A_M dt$. One can easily verify that the above defined quantities satisfy the usual Bianchi identity, that is Eq. (11) with vanishing RHS, and that, as a consequence, $\tilde{\rho}_M \sim \tilde{a}^{-3(1+w_M)}$. The expansion rate, $H_{ST} \equiv d \log \tilde{a} / d\tilde{t}$, is given by

$$H_{ST} = \frac{1 + \alpha_M(\varphi) \varphi'}{A_M(\varphi)} \frac{\dot{a}}{a}, \quad (15)$$

where we have defined α_M according to Eq. (10), and $(\cdot) \equiv d(\cdot) / d \log a$. Using (15) and (14) in (8), we obtain the Friedmann equation in the ST theory,

$$H_{ST}^2 = \frac{A_M^2(\varphi)}{3M_*^2} \frac{(1 + \alpha_M(\varphi) \varphi')^2}{1 - (\varphi')^2/6} \left[\tilde{\rho}_M + \tilde{V} \right], \quad (16)$$

where $\tilde{V} \equiv A_M^{-4} V$. Comparing to Eq.(1), we see that apart from the extra contribution to $\tilde{\rho}_{tot}$ from the scalar field potential, the ST Friedmann equation differs from the standard one of GR by the presence of an effective, field-dependent Planck mass,

$$\frac{1}{3M_p^2} \rightarrow \frac{A_M^2(\varphi)}{3M_*^2} \frac{(1 + \alpha_M(\varphi) \varphi')^2}{1 - (\varphi')^2/6} \simeq \frac{A_M^2(\varphi)}{3M_*^2}, \quad (17)$$

where the last equality holds with very good approximations for all the choices of A_i functions considered in the present paper.

If the conformal factor $A_M^2(\varphi)$ is constant, then the full action $S_g + S_M$ is just that of GR (with $M_p = M_*/A_M$) plus a minimally coupled scalar field. Therefore, the coupling function α_M , defined according to Eq. (10), measures the “distance” from GR of the ST theory, $\alpha_M = 0$ being the GR limit. Changing A_M , and, therefore, changing the effective Planck mass, opens the way to a modification of the standard relation between H and $\tilde{\rho}$, or T . In order to study the evolution of $A_M(\varphi)$, one should come back to Eq. (9). Considering an initial epoch deeply inside radiation domination, we can neglect the

contribution from the potential on the RHS. The other contribution, the trace of the energy-momentum tensor ($\rho_M - 3p_M$) is zero for fully relativistic components but turns on to positive values each time the temperature drops below the mass threshold of a particle in the thermal bath. Assuming a mass spectrum – *e.g* that of the SM, or of the MSSM – one finds that this effect is effective enough to drive the scalar field evolution even in the radiation domination era [7].

The key point to notice is that if there is a field value, φ_0 , such that $\alpha_M(\varphi_0) = 0$, this is a *fixed point* of the field evolution [8, 9]. Moreover, if α'_M is positive (negative) the fixed point is attractive (repulsive). Since $\alpha_M = 0$ corresponds to the GR limit, we see that GR is a – possibly attractive – fixed point configuration.

The impact on the DM relic abundance of a scenario based on this mechanism of attraction towards GR was considered in [7, 10]. Regardless of the particular form of the $A_M(\varphi)$ function, the requirement that an attractive fixed point towards GR exists implies that the effective Planck mass in the past was *not smaller* than today, that is to say that, at a certain temperature T , for instance at DM freeze out, the universe was expanding *not more slowly* than in the standard GR case. This is easy to understand, since the past values of φ , and then of $A_M(\varphi)$ are all such that

$$\log \frac{A_M(\varphi)}{A_M(\varphi_0)} = \int_{\varphi_0}^{\varphi} dx \alpha_M(x) > 0, \quad (18)$$

with φ between φ_0 and the next fixed point. Therefore, according to Eq. (17), the ratio between H_{ST} and H_{GR} ,

$$\frac{H_{ST}}{H_{GR}} \simeq A_M^2(\varphi), \quad (19)$$

can only decrease in time. Another way of seeing this, is by noticing that the RHS of the field equation (9), is proportional to the field derivative of the effective potential $V_{\text{eff}} = \rho_M + V$, where the field dependence of ρ_M is given by Eq. (12). Then, neglecting again V , the field evolution will tend towards minimizing $A_M(\varphi)$ (if $w_M \leq 1/3$), therefore minimizing H_{ST}/H_{GR} .

Eq. (19) is obtained under the same approximation used in Eq. (17), that is by neglecting the scalar field contribution to the total energy density, and assuming the same matter content in the ST and GR cases. Notice that these approximations are far from mandatory, and we only use them here in order to illustrate how the fixed point mechanism works. The numerical analysis we will present in the following were indeed obtained using the full expressions, such as Eq. (16). Finally, in order to identify the fixed point with GR, we have to impose

$$\frac{1}{3M_p^2} = \frac{A_M^2(\varphi_0)}{3M_*^2}. \quad (20)$$

B. Lowering H in the past

All the mechanisms discussed so far (*i.e.* adding relativistic d.o.f.’s, the kination scenario, or ST theories with a single matter sector) give a faster expansion of the universe in the past w.r.t. the standard case. In the case of ST theories with a single matter sector, we have just seen that this comes as a consequence of the requirement of an attractive fixed point towards GR. In this subsection, we will show that adding more matter sectors, with different conformal factors, allows us to keep the desirable property of late time convergence to GR and, at the same time, to have a lower expansion rate in the past. To illustrate this point, we will consider just two matter sectors, a “visible” one, containing the SM or one of its extensions, and a “hidden” one. The full action is then given by

$$S = S_g + S_v + S_h, \quad (21)$$

where the two matter actions S_v and S_h have two different conformal functions $A_v(\varphi)$ and $A_h(\varphi)$. The discussion follows quite closely that of the previous subsection. The only subtle point is to notice that, if $A_v(\varphi) \neq A_h(\varphi)$ there is no Weyl transformation that gives covariantly conserved energy-momentum tensors both for the visible and for the hidden sector. Since particle masses, reaction rates and so on, are computed in terms of parameters of the “visible” action, the transformation to perform in order to compare with the standard GR case is the one leading to a conserved $\tilde{T}_{\mu\nu}^v$, that is [4]

$$\tilde{g}_{\mu\nu} = A_v^2(\varphi) g_{\mu\nu}, \quad (22)$$

and so on. As a consequence, the expansion rate in this case is given by

$$H_{ST}^2 = \frac{A_v^2(\varphi)}{3M_*^2} \frac{(1 + \alpha_v(\varphi) \varphi')^2}{1 - (\varphi')^2/6} \left[\tilde{\rho}_v + \tilde{\rho}_h + \tilde{V} \right], \quad (23)$$

where

$$\tilde{\rho}_v \sim \tilde{a}^{-3(1+w_v)},$$

while

$$\tilde{\rho}_h \sim \tilde{a}^{-3(1+w_h)} \left(\frac{A_h}{A_v} \right)^{1-3w_h}.$$

In order to study the existence of a fixed point, it is still convenient to revert to the Einstein Frame field equation, Eq. (9). The RHS, is now given by the field derivative of the effective potential

$$V_{\text{eff}} = \rho_v + \rho_h + V, \quad (24)$$

with the field-dependence of $\rho_{v,h}$ given by Eq. (12). The condition to have a fixed point is then

$$\sum_{i=v,h} \alpha_i (1 - 3w_i) \rho_i + V' = 0, \quad (25)$$

while, asking that the fixed point is stable implies

$$\sum_{i=v,h} (\alpha'_i (1 - 3w_i) \rho_i + \alpha_i^2 (1 - 3w_i)^2 \rho_i + V'') \geq 0. \quad (26)$$

From Eq. (23) we see that, away from the fixed point, H_{ST} is lower than the one obtained in GR with the same matter content but frozen scalar fields if

$$\frac{d^2}{d\varphi^2} \left(A_v^2(\varphi) \frac{1 + \tilde{\rho}_h/\tilde{\rho}_v|_{ST}}{1 + \tilde{\rho}_h/\tilde{\rho}_v|_{GR}} \right) < 0, \quad (27)$$

where, again, we have assumed that the second fraction in Eq. (23) is approximately one, and we have neglected the contribution from the scalar potential.

As an example, we now consider A_i functions of the form

$$A_{v,h}(\varphi) = 1 + b_{v,h} \varphi^2. \quad (28)$$

Neglecting again the potential, we see that the fixed point condition, Eq. (25), is solved by the symmetric point $\varphi = 0$. The stability condition, Eq. (26), translates into

$$\sum_{i=v,h} b_i (1 - 3w_i) \rho_i \geq 0, \quad (29)$$

which, according to Eq. (27), is compatible with a lower H_{ST}/H_{GR} outside the fixed point (*i.e.* in the past), if

$$b_v < 0, \quad (30)$$

where we have assumed $\rho_h \ll \rho_v$ close to the fixed point, since we are interested in a physical situation in which most of the dark matter lives in the “visible” sector (as in the MSSM).

C. Numerical examples

To be implemented in a sensible cosmological model, the previously discussed mechanism for lowering the expansion rate in the past has to respect the severe bound coming from BBN, namely [11]

$$\frac{|H_{ST} - H_{GR}|}{H_{ST}} < 10\% \quad \text{at BBN.} \quad (31)$$

We now show in a few examples that indeed the bound (31) can be satisfied even by points of the parameters space (b_v, b_h, φ_{in}) giving rise to a pre-BBN value of the ratio (19) as low as 10^{-3} . Such important deviations from standard cosmology are allowed in the present scenario by the effectiveness of the GR fixed point.

In order to numerically solve Eqs. (7–9) we need the equation of state parameters

$$1 - 3w_i(y) = \frac{I_i(y)}{1 + e^{y - y_{eq}^i}} + \frac{1}{e^{y_{eq}^i - y} + 1} \quad i = v, h \quad (32)$$

where $y = \log \tilde{a}$ and y_{eq}^i refers to the equivalence in the visible ($i = v$) and hidden ($i = h$) sectors respectively. The functions $I_i(y)$ are given by [7]

$$I_i(y) = \sum_{P_i} \frac{15}{\pi^2} \frac{g_{P_i}}{g_i} e^{2(y - y_{P_i})} \times \int_0^{+\infty} \frac{z_{P_i}^2 dz_{P_i}}{\sqrt{e^{2(y - y_{P_i})} + z_{P_i}^2} \left[e^{\sqrt{e^{2(y - y_{P_i})} + z_{P_i}^2}} \pm 1 \right]} \quad (33)$$

where $y_{P_i} = -\log m_{P_i}/T_0$, m_{P_i} and g_{P_i} are the masses and the relativistic degrees of freedom of the particles P_i and $T_0 = 2.73$ K $\simeq 2.35 \times 10^{-13}$ GeV is the current temperature of the Universe.

As mass thresholds for the visible sector, namely y_{P_v} , we use the one given by a MSSM-like mass spectrum [36] while the equivalence time y_{eq}^v has been computed according to [12]. The analogous quantities for the hidden sector are free parameters of the theory that nevertheless do not have any drastic impact on the final result. The only significant assumption we do is that $\lim_{y \rightarrow \bar{y}} (1 - 3w_h(y)) \simeq 1$ for $\bar{y} \ll y_{BBN}$. In such a way the contribution of the hidden sector to the RHS of the scalar field equation before BBN can be dominant w.r.t. the one of the visible sector. The equation of state parameter w_h is plotted in Fig. (1) for three different values of y_{eq}^h . In Fig. (2) instead, for a given value of y_{eq}^h we plot w_h for three different choices of mass thresholds in the hidden sector.

We can now integrate the equation of motion for the scalar field. Fixing as the initial condition $\varphi_{in} = 1$ (in Planck units), we show in Fig. (3) the behavior of φ as a function of y for three different choices of parameters b_v and b_h . For the same choices we plot in Figs. (4) and (5) the evolution of the ratio H_{ST}^2/H_{GR}^2 and of the function α_v respectively. As anticipated, an agreement with the BBN bound is achieved even by solutions with a pre-BBN value of the ratio H_{ST}^2/H_{GR}^2 of order 10^{-3} .

The scalar field dynamics can be qualitatively understood by having in mind the following rough estimation for its first derivative

$$\dot{\varphi} \propto - \sum_i \alpha_i (1 - 3w_i) \rho_i, \quad (34)$$

where each α_i is weighted by the the corresponding function $(1 - 3w_i) \rho_i$. If both α_i are positive, the scalar field is driven toward the fixed point $\phi = 0$. Analogously, negative values of the couplings α_i lead to a run-away behavior of φ . The present scenario corresponds to the case in which (before BBN) $\alpha_v < 0$ and $\alpha_h > 0$. Therefore, the interplay between the contributions of the hidden and visible sectors to the RHS of Eq. (34) becomes relevant. If at early time $(1 - 3w_h) \rho_h$ always dominates, then the only effect of having a $\alpha_v < 0$ is to realize the initial condition $H_{ST}^2/H_{GR}^2 < 1$ (see Subsection IB). This is the case in Models 1 and 2 in Fig. (4). However, if at early time there is a short period where the visible

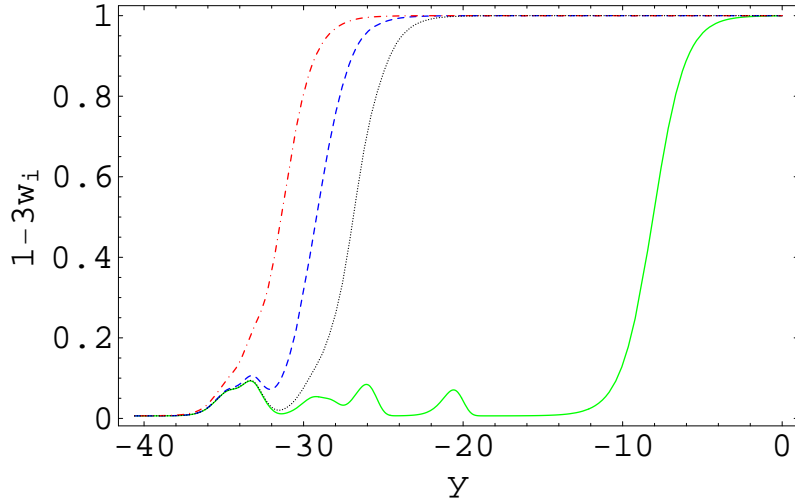


FIG. 1: Four different combinations of the quantity $(1 - 3w_i)$ as a function of y . For all of them a MSSM-like mass spectrum is assumed (heaviest mass 1 TeV). The solid [green] line corresponds to the visible sector; the dot-dashed [red], dashed [blue] and dotted [black] lines represent a hidden sector with a hidden matter-hidden radiation equivalence at 10 GeV, 1 GeV and 0.1 GeV respectively.

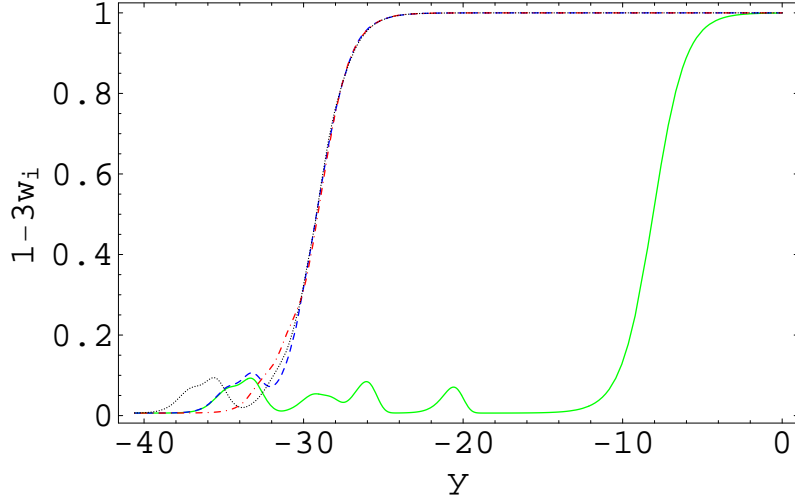


FIG. 2: Four different combinations of the quantity $(1 - 3w_i)$ as a function of y . The solid [green] line corresponds to the visible sector with a MSSM-like mass spectrum (heaviest mass 1 TeV). The dot-dashed [red], dashed [blue] and dotted [black] lines represent a hidden sector with three different mass spectra: heaviest mass 0.1 TeV, 1 TeV and 10 TeV respectively. In the hidden sector the equivalence temperature is fixed at 1 GeV.

sector contribution $(1 - 3w_v)\rho_v$ dominates, then the ratio H_{ST}^2/H_{GR}^2 decreases from its initial value until when $(1 - 3w_v) \simeq 1$ and, as a consequence, the hidden sector contribution becomes dominant. This happens in Model 3 of Fig. (4) where the parameter b_v has been tuned close to $-1/2$ [37].

Let us conclude this subsection with an estimation of the dependence of our results from the parameters b_v . According to [13], the level of fine-tuning Δ_λ on a parameter λ needed to get the required value of an observable \mathcal{O} is given by $\Delta_\lambda = |(\lambda/\mathcal{O})(\partial\mathcal{O}/\partial\lambda)|$. Requiring at early time (when $\varphi \sim 1$) $\mathcal{O} = H_{ST}^2/H_{GR}^2 \simeq 10^{-3}$ and

choosing $\lambda = b_v \sim -1/2$ we find

$$\Delta_{b_v} \sim 2|(1 + b_v)b_v|10^3 \sim 5 \times 10^2. \quad (35)$$

Therefore, configurations with a small initial value of H_{ST}^2/H_{GR}^2 are very sensitive to the parameter b_v .

II. IMPLICATIONS FOR DARK MATTER IN THE CMSSM

A modification of the Hubble rate at early times has impact on the formation of dark matter as a thermal

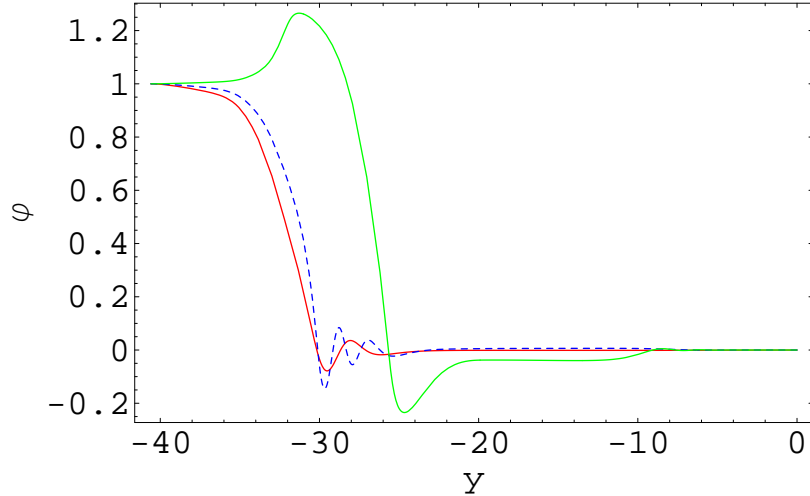


FIG. 3: Evolution of the scalar field φ with y for three different choices of the parameters (b_v, b_h) . The dark solid [red], dashed [blue] and light solid [green] lines correspond respectively to $(-0.2, 5)$ [Model 1], $(-0.4, 15)$ [Model 2] and $(-0.521, 50)$ [Model 3]. BBN occurs at $y \simeq -22$.

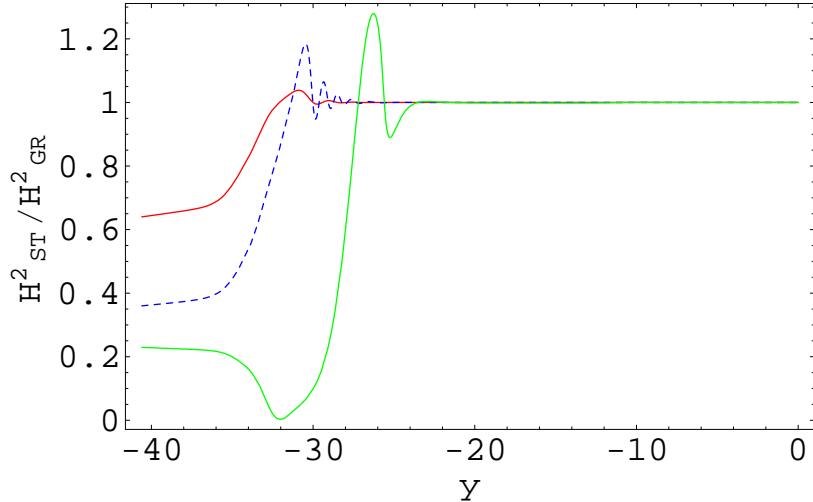


FIG. 4: Ratio of the ST and GR Hubble rates squared H_{ST}^2/H_{GR}^2 as a function of y for three different choices of parameters (b_v, b_h) . The dark solid [red], dashed [blue] and light solid [green] lines correspond respectively to $(-0.2, 5)$ [Model 1], $(-0.4, 15)$ [Model 2] and $(-0.521, 50)$ [Model 3]. BBN occurs at $y \simeq -22$.

relic, if the particle freeze-out occurs during the period of modification of the expansion rate. ST cosmologies with a Hubble rate increased with respect to the GR case have been discussed in Refs. [7, 10, 14], where the effect on the decoupling of a cold relic was discussed and bounds on the amount of increase of the Hubble rate prior to Big Bang Nucleosynthesis have been derived from the indirect detection signals of dark matter in our Galaxy. For cosmological models with an enhanced Hubble rate, the decoupling is anticipated, and the required amount of cold dark matter is obtained for larger annihilation cross-sections: this, in turn, translates into larger indirect detection rates, which depend directly on the annihilation process. In Refs. [10, 14] we discussed

how low-energy antiprotons and gamma-rays fluxes from the galactic center can pose limits on the admissible enhancement of the pre-BBN Hubble rate. We showed that these limits may be severe: for dark matter particles lighter than about a few hundred GeV antiprotons set the most important limits, which are quite strong for dark matter masses below 100 GeV. For heavier particles, gamma-rays are more instrumental in determining significant bounds. Further recent considerations on the effect of cosmologies with modified Hubble rate are discussed in Refs. [15, 16, 17, 18, 19, 20].

In the case of the cosmological models which predict a reduced Hubble rate, the situation is opposite: a smaller expansion rate implies that the cold relic particle remains

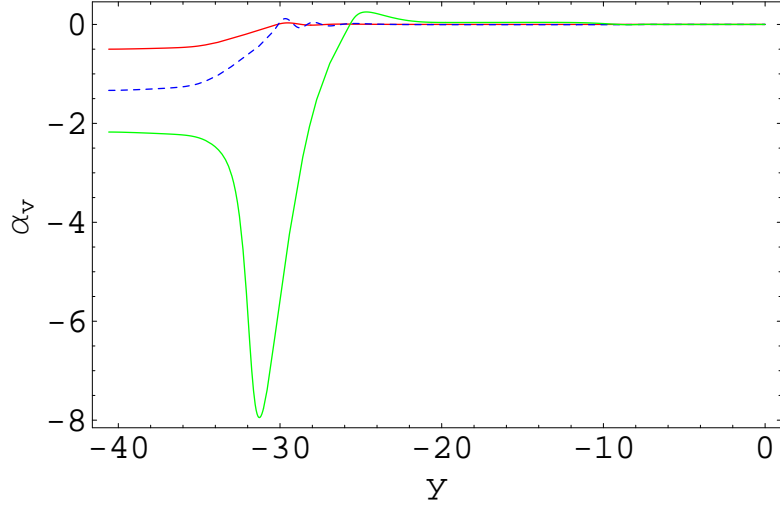


FIG. 5: Evolution of the coupling function α_v with y for three different choices of parameters (b_v, b_h) . The dark solid [red], dashed [blue] and light solid [green] lines correspond respectively to $(-0.2, 5)$ [Model 1], $(-0.4, 15)$ [Model 2] and $(-0.521, 50)$ [Model 3]. The BBN occurs at $y \simeq -22$

in equilibrium for a longer time in the early Universe, and, as a consequence, its relic abundance turns out to be smaller than the one obtained in GR. In this case, the required amount of dark matter is obtained for smaller annihilation cross sections, and therefore indirect detection signals are depressed as compared to the standard GR case: as a consequence, no relevant bounds on the pre-BBN expansion rate can be set. On the other hand, for those particle physics models which typically predict large values for the relic abundance of the dark matter candidate, this class of ST cosmologies may have an important impact in the selection of the regions in parameter space which are cosmologically allowed.

A typical and noticeable case where the relic abundance constraint is very strong is offered by minimal SUGRA models, where the neutralino is the dark matter candidate and its relic abundance easily turns out to be very large, in excess of the cosmological bound provided by WMAP [12]:

$$0.092 \leq \Omega_{\text{CDM}} h^2 \leq 0.124 \quad (36)$$

Large sectors of the supersymmetric parameter space are excluded by this bound. A reduction of the expansion rate will therefore have a crucial impact on the allowed regions in parameter space, which are therefore enlarged. The potential reach of accelerators like the Large Hadron Collider (LHC) or the International Linear Collider (ILC) on the search of supersymmetry may therefore be affected by this broadening of the allowed parameter space, especially for the interesting situation of looking for supersymmetric configurations able to fully explain the dark matter problem.

We have therefore studied how the allowed parameter space of minimal SUGRA changes in ST cosmologies with a reduced Hubble rate. We have used a cosmological model of the type of Model 3 discussed in the

previous Section and depicted in Fig. 4. For the calculations of the neutralino relic density we have used the DarkSUSY package [21], with an interface to ISAJET 7.69 [22] for the minimal SUGRA parameter space determination, with two major modifications. First, the relic density is obtained by the implementation of a numerical solution of a modified Boltzmann equation which includes the reduced Hubble rate evolution (similar to the method used in Refs. [7, 10, 14] for the enhanced case). Second, the NNLO contributions to the Standard Model branching ratio of the $\text{BR}[\bar{B} \rightarrow X_s \gamma]$ have been recently determined [23]: the updated result, which we use here, is $\text{BR}[\bar{B} \rightarrow X_s \gamma]_{\text{SM}} = (3.15 \pm 0.23) \times 10^{-4}$ ($E_\gamma > 1.6$ GeV). In order to implement the NNLO SM result with the supersymmetric contribution, which are known up to the NLO [24], we have used the following approximate expression, which is suitable when the beyond-standard-model (BSM) corrections are small [23, 25, 26]:

$$\begin{aligned} [\text{BR}]_{\text{theory}} \times 10^4 &= 3.15 & (37) \\ &- 8.0 \times \left(\delta_{\text{BSM}}[C_7^{(0)}] + \frac{\alpha_s(\mu_0)}{4\pi} \delta_{\text{BSM}}[C_7^{(1)}] \right) \\ &- 1.9 \times \left(\delta_{\text{BSM}}[C_8^{(0)}] + \frac{\alpha_s(\mu_0)}{4\pi} \delta_{\text{BSM}}[C_8^{(1)}] \right) \end{aligned}$$

where $C_i^{(j)}(\mu_0)$ are LO ($j = 0$) and NLO ($j = 1$) Wilson coefficients. For the matching scale μ_0 (which should be taken as $\mu_0 = 2M_W \sim 160$ GeV) we use $\mu_0 = \bar{m}_t(m_{t,\text{pole}}) = 163.7$ GeV, and we use a top-quark pole mass $m_{t,\text{pole}} = 171.4$ GeV [27] and $\alpha_s(M_Z) = 0.1189$ [28]. The theoretical calculation in Eq. (37) is compared to the current world average of the experimental determination [29]:

$$[\text{BR}]_{\text{exp}} \times 10^4 = \left(3.55 \pm 0.24 \begin{array}{l} +0.09 \\ -0.10 \end{array} \pm 0.03 \right) \quad (38)$$

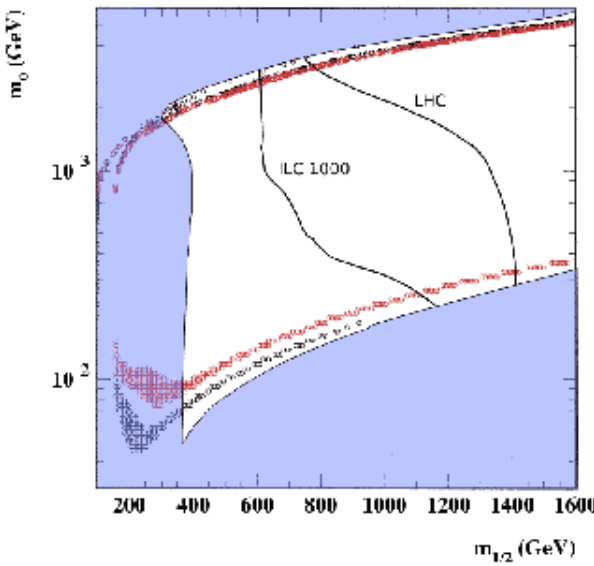


FIG. 6: Regions in the $(m_{1/2}, m_0)$ parameter space where the neutralino relic abundance falls in the cosmological interval for cold dark matter obtained by WMAP, for $\tan\beta = 10$, $A_0 = 0$ and positive μ . In the bulk region, the lower [black] points refer to GR cosmology, while the upper [red] points stand for a ST cosmology with a reduced Hubble rate. The shaded areas are forbidden by theoretical arguments and experimental bounds. The two curves are indicative of the reach for 100 fb^{-1} of the LHC [33, 34] and of the ILC at $\sqrt{s} = 1000$ GeV energy [33, 35].

The estimated error of the theoretical calculation of the Standard Model contribution is $\pm 0.23 \times 10^{-4}$ [23, 25]. For the theoretical beyond-SM correction we have assumed an error of the same size. Adding all experimental and theoretical errors we get the following 2σ interval for the branching ratio:

$$2.71 \times 10^{-4} \leq \text{BR}[\bar{B} \rightarrow X_s \gamma] \leq 4.39 \times 10^{-4} \quad (39)$$

Supersymmetric models for which the theoretical calculation in Eq. (37) is outside this interval are considered in disagreement with the experimental result.

A. Low $\tan\beta$

As a first example, we scan the universal gaugino mass $m_{1/2}$ and soft scalar-mass m_0 parameters of minimal SUGRA for a low value of the $\tan\beta$ parameter ($\tan\beta$ is defined, as usual, as the ratio of the two Higgs vacuum expectation values v_2 and v_1 , where v_2 (v_1) gives mass to the top(down)-type fermions) and a vanishing universal trilinear coupling A_0 . The higgs-mixing parameter μ , derived by renormalization group equation (RGE) evolution and electro-weak symmetry breaking (EWSB) conditions, is taken as positive. Our choice of parameters is

here:

$$\tan\beta = 10 \quad \text{sgn}(\mu) = + \quad A_0 = 0 \quad (40)$$

Fig. 6 shows the result in the plane $(m_{1/2}, m_0)$, both for the standard GR case and for the ST case of Model 3. Shaded areas denote regions which are excluded either by theoretical arguments or by experimental constraints on higgs and supersymmetry searches, as well as supersymmetric contributions to rare processes, namely to the $\text{BR}[\bar{B} \rightarrow X_s \gamma]$ and to the muon anomalous magnetic moment $(g-2)_\mu$. More specifically, the upper wedge refers to the non-occurrence of the radiative EWSB and the lower-right area to the occurrence of a stau LSP. The low- $m_{1/2}$ vertical band is excluded by the quoted experimental bounds.

The sector of the supersymmetric parameter space which provides LSP neutralinos with a relic abundance in the cosmological range of Eq. (36) are denoted by the open circles: in the so-called “bulk region” (low values of both $m_{1/2}$ and m_0), the lower [black] points fulfill the density constraint in the standard GR cosmology, while the upper [red] points in the modified ST cosmology with reduced Hubble rate. In the region above the points, the neutralino relic abundance exceeds the cosmological bounds, and therefore refers to supersymmetric configurations which are excluded by cosmology. Fig. 6 shows that in our modified cosmological scenario, the allowed regions in parameter space are enlarged (the relic density has been decreased 1.4 times to 4.4 times compared to the standard case) and those which refer to dominant neutralino dark matter are shifted towards larger values of the supersymmetric parameters $m_{1/2}$ and m_0 . The bulk region now occurs for values of m_0 larger by a factor of 2 (while the bulk region for the GR case now refers to cosmologically subdominant neutralinos). Nevertheless, this sector of the parameter space is already mostly excluded by accelerator searches. In the coannihilation channel, which extends for low values of the ratio $m_0/m_{1/2}$, along the boundary of the stau excluded region, the change is more dramatic: this coannihilation region, which appears to be fully explorable at the LHC, now extends towards larger values of $m_{1/2}$, beyond the estimated LHC reach.

In the cosmologically allowed region of large m_0 , where a gaugino-mixing becomes possible and therefore the neutralino can efficiently annihilate and provide an acceptable relic abundance (a mechanism discussed in Ref. [30] and lately dubbed as “focus point region” in Ref. [31]), the effect of reducing the Hubble rate translates into a slight lowering of the cosmologically relevant region, with no drastic phenomenological effect in this case.

B. Large $\tan\beta$

As a second example, we consider the case of large values of $\tan\beta$. We show two cases, one which refers to a negative μ parameter:

$$\tan\beta = 45 \quad \text{sgn}(\mu) = - \quad A_0 = 0 \quad (41)$$

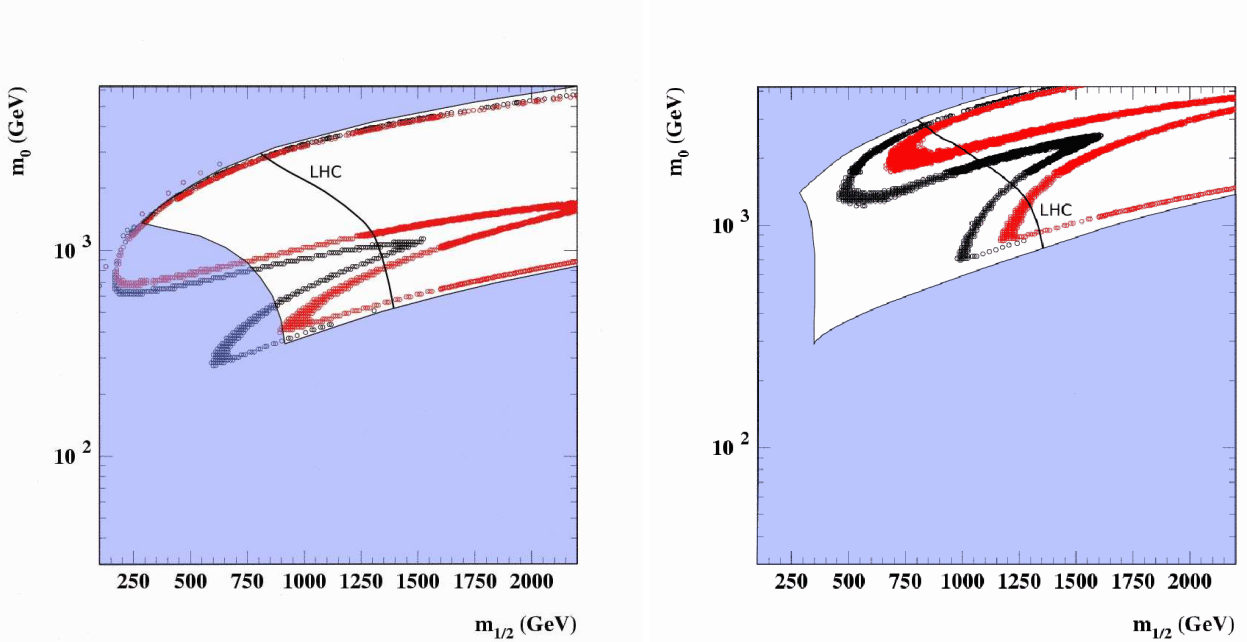


FIG. 7: Regions in the $(m_{1/2}, m_0)$ parameter space where the neutralino relic abundance falls in the cosmological interval for cold dark matter obtained by WMAP. The left panel refers to $\tan \beta = 45$, $A_0 = 0$ and negative μ . The right panel is obtained for $\tan \beta = 53$, $A_0 = 0$ and positive μ . Notations are as in Fig. 6.

and one to a positive value of μ :

$$\tan \beta = 53 \quad \text{sgn}(\mu) = + \quad A_0 = 0 \quad (42)$$

The results are shown in Fig. 7. In this case the change in the cosmological scenario is more relevant, not only in the coannihilation channel, but also in the “funnel” region [32] which occurs for intermediate values of the ratio $m_0/m_{1/2}$. In the GR case, almost the full cosmologically allowed parameter space may be explored by the LHC. When the ST cosmology is considered, the funnel region dramatically extends towards large values of m_0 and $m_{1/2}$ and goes well beyond the accelerators reach. Also the coannihilation region now extends to values of $m_{1/2}$ well in excess of 2 TeV. In the case of the positive μ reported in the right panel of Fig. 7, also the focus-point region shows a deviation from the GR case, and is shifted towards lower values of the m_0 parameter. In summary, for these large values of $\tan \beta$ the reach of LHC on the cosmologically relevant configurations is less strong than in the case of GR: a discover of supersymmetry will be more likely related to a subdominant neutralino dark matter.

III. CONCLUSIONS

We have discussed Scalar Tensor cosmologies by determining under what conditions these theories can predict an expansion rate which is reduced as compared to the standard General Relativity case. We showed that in the

case of ST theories with a single matter sector, the typical behaviour is an enhancement of the Hubble rate in the past: this arises as a consequence of the requirement of an attractive fixed point towards GR at late times. Instead, when additional matter sectors, with different conformal factors, are added, we can maintain the desirable property of late time convergence to GR and, at the same time, obtain a reduced expansion rate in the past. We showed that, for suitable choices of the parameters which govern the scalar field evolution, a sizeable reduction (up to about 2 orders of magnitude) of the Hubble rate prior to Big Bag Nucleosynthesis can be obtained. Large reductions come along with some fine-tuning on the scalar field parameters, while a milder decrease occurs without tuning problems.

We have then applied the results obtained on the reduction of the early-time Hubble rate to the formation of dark matter and the determination of its relic abundance. If the dark matter decouples during the period of Hubble-rate reduction, the relic abundance turns out to be reduced as compared to the standard GR case. This has therefore impact on the determination of the cosmologically allowed parameter space in minimal SUGRA models, where, in large portions of the parameter space and for the GR case, the neutralino relic abundance is large and in excess of the WMAP bound. We have therefore explicitly shown what are the modifications to the minimal SUGRA allowed parameter space when ST cosmologies with a reduced Hubble rate are considered and we have quantified the effect in view of the reach of LHC and ILC on the searches for supersymmetry at future ac-

celerators. These modifications move the cosmologically relevant regions up to a few TeV for the $m_{1/2}$ parameters, since they significantly extend the coannihilation corridor and the funnel region which occurs at large values of $\tan\beta$.

Acknowledgments

We thank P. Gambino for useful discussions concerning the new implementation of the recent theoretical developments on the $b \rightarrow s + \gamma$ branching ratio. We ac-

knowledge Research Grants funded jointly by the Italian Ministero dell’Istruzione, dell’Università e della Ricerca (MIUR), by the University of Torino and by the Istituto Nazionale di Fisica Nucleare (INFN) within the *Astroparticle Physics Project*. This research was supported in part by the European Communitys Research Training Networks under contracts MRTN-CT-2004-503369 and MRTN-CT-2006-035505. N.F. wishes to warmly thank the Astroparticle and High Energy Group of the IFIC/Universitat de València for the hospitality during the completion of this work.

[1] E.W. Kolb and M.S. Turner, “The Early Universe” 1990 Addison–Wesley Publishing Company.

[2] P. Salati, Phys. Lett. B **571**, 121 (2003) [arXiv:astro-ph/0207396].

[3] P. Jordan, *Schwerkraft und Weltall* (Vieweg, Braunschweig, 1955); Nature (London), **164**, 637 (1956); M. Fierz, Helv. Phys. Acta **29**, 128 (1956); C. Brans and R.H. Dicke, Phys. Rev. **124**, 925 (1961).

[4] R. Catena, M. Pietroni and L. Scarabello, Phys. Rev. D **70**, 103526 (2004) [arXiv:astro-ph/0407646].

[5] S. S. Gubser and P. J. E. Peebles, **MANCA REF**

[6] R. Catena, M. Pietroni and L. Scarabello, Phys. Rev. D **76**, 084039 (2007) [arXiv:astro-ph/0604492]. Phys. Rev. D **70**, 123510 (2004); Phys. Rev. D **70**, 123511 (2004).

[7] R. Catena, N. Fornengo, A. Masiero, M. Pietroni and F. Rosati, Phys. Rev. D **70**, 063519 (2004).

[8] T. Damour and A. M. Polyakov, Nucl. Phys. B **423**, 532 (1994); Gen. Rel. Grav. **26**, 1171 (1994).

[9] N. Bartolo and M. Pietroni, Phys. Rev. D **61**, 023518 (2000).

[10] M. Schelke, R. Catena, N. Fornengo, A. Masiero and M. Pietroni, Phys. Rev. D **74**, 083505 (2006).

[11] E. Lisi, S. Sarkar and F. L. Villante, Phys. Rev. D **59**, 123520 (1999) [arXiv:hep-ph/9901404]. K. A. Olive and D. Thomas, Astropart. Phys. **11**, 403 (1999) [arXiv:hep-ph/9811444].

[12] D. N. Spergel *et al.* [WMAP Collaboration], Astrophys. J. Suppl. **170**, 377 (2007) [arXiv:astro-ph/0603449].

[13] R. Barbieri and G. F. Giudice, Nucl. Phys. B **306**, 63 (1988).

[14] F. Donato, N. Fornengo and M. Schelke, JCAP **0703** (2007) 021 [arXiv:hep-ph/0612374].

[15] E. Abou El Dahab and S. Khalil, JHEP **0609** (2006) 042 [arXiv:hep-ph/0607180].

[16] C. Pallis, arXiv:hep-ph/0610433.

[17] M. Drees, H. Iminniyaz and M. Kakizaki, Phys. Rev. D **76** (2007) 103524 [arXiv:0704.1590 [hep-ph]].

[18] D. J. H. Chung, L. L. Everett and K. T. Matchev, Phys. Rev. D **76** (2007) 103530 [arXiv:0704.3285 [hep-ph]].

[19] D. J. H. Chung, L. L. Everett, K. Kong and K. T. Matchev, JHEP **0710** (2007) 016 [arXiv:0706.2375 [hep-ph]].

[20] E. J. Chun and S. Scopel, JCAP **0710** (2007) 011 [arXiv:0707.1544 [astro-ph]].

[21] P. Gondolo, J. Edsjo, P. Ullio, L. Bergström, M. Schelke and E. Baltz, JCAP **07** (2004) 008 [astro-ph/0406204] (<http://www.physto.se/~edsjo/darksusy/>)

[22] F.E. Paige, S.D. Protopopescu, H. Baer and X. Tata [arXiv:hep-ph/0312045]; H. Baer, F.E. Paige, S.D. Protopopescu, and X. Tata, ISAJET (<http://www.hep.fsu.edu/~isajet/>)

[23] M. Misiak *et al.*, Phys. Rev. Lett. **98** (2007) 022002 [arXiv:hep-ph/0609232].

[24] G. Degrassi, P. Gambino and G. F. Giudice, JHEP **0012** (2000) 009; M. Ciuchini, G. Degrassi, P. Gambino and G. F. Giudice, Nucl. Phys. **B534** (1998) 3.

[25] M. Misiak and M. Steinhauser, Nucl. Phys. **B764** (2007) 62 [arXiv:hep-ph/0609241].

[26] M. Misiak and M. Steinhauser, private communication; P. Gambino, private communication.

[27] E. Brubaker *et al.* [Tevatron Electroweak Working Group], arXiv:hep-ex/0608032.

[28] Particle Data group (W. M. Yao *et al.*), J. Phys. G**33** (2006) 1; S. Bethke, Prog. Part. Nucl. Phys. **58** (2007) 351 [arXiv:hep-ex/0606035].

[29] E. Barberio *et al.* [Heavy Flavor Averaging Group (HFAG) Collaboration], arXiv:0704.3575 [hep-ex]

[30] V. Berezinsky, A. Bottino, J. R. Ellis, N. Fornengo, G. Mignola and S. Scopel, Astropart. Phys. **5**, 1 (1996) [arXiv:hep-ph/9508249].

[31] J. L. Feng, K. T. Matchev and T. Moroi, Phys. Rev. Lett. **84** (2000) 2322 [arXiv:hep-ph/9908309].

[32] J. R. Ellis, T. Falk, G. Ganis, K. A. Olive and M. Srednicki, Phys. Lett. B **510** (2001) 236 [arXiv:hep-ph/0102098]; J. R. Ellis, K. A. Olive, Y. Santoso and V. C. Spanos, Phys. Lett. B **565** (2003) 176 [arXiv:hep-ph/0303043].

[33] G. Weiglein *et al.* [LHC/LC Study Group], Phys. Rept. **426** (2006) 47 [arXiv:hep-ph/0410364].

[34] H. Baer, C. Balazs, A. Belyaev, T. Krupovnickas and X. Tata, JHEP **0306** (2003) 054 [arXiv:hep-ph/0304303].

[35] H. Baer, A. Belyaev, T. Krupovnickas and X. Tata, JHEP **0402** (2004) 007 [arXiv:hep-ph/0311351].

[36] Only particles with a mass smaller than the temperature of the phase transition by means of which they become massive have to be considered (see also [7] and references therein).

[37] With an initial condition $\varphi_{in} = 1$, smaller values of b_v would lead to a divergent value of α_v during the evolution of φ .